

SINGLE AND MULTI-RESPONSE OPTIMIZATION FOR LASER MICROMACHINING OF AL 7075 ALLOY

Samrat Choudhury¹, Kajal Kumar Mandal²

Department of Mechanical Engineering, NERIST, Itanagar-791109, India.

Email: ¹samratchoudhury72@gmail.com, ²kkm@nerist.ac.in

Paper submitted on August 17 2022, Accepted after revision on June 05 2023
DOI: 10.21843/reas/2022/39-47/222962

Abstract: Al 7075 alloy is one of the strongest aluminium alloys having good fatigue strength and durability property. Its density is of 2.810 g/cm³. Zinc is the primary alloying element along with other elements such as magnesium, copper, chromium, iron and other elements. Innovative material development, strict design criteria, and complicated and entangled work sizes necessitate the use of non-traditional machining techniques. One such method for sculpting a wide variety of engineering materials is laser micro-machining. In present research, laser micro-machining is conducted on Al 7075 alloy. The Design of experiment (DoE) is performed using Response Surface Methodology (RSM). Here, Kerf Width (KW) and heat affected zone (HAZ) are investigated by varying Laser Beam Power (LBP), Pulse Frequency (PF) and Scanning Speed (SS). Regression models for KW and HAZ are generated to observe the effects of process parameters. Also, using RSM, both single and multi-objective optimization is performed.

Keywords: Laser Micro-machining, Al 7075 Alloy, Response Surface Method, Regression Model, Optimization.

1. INTRODUCTION

Al 7075 alloy is a strong material which can be compared to any type of steel, having good fatigue strength and average machinability. As it has significantly better corrosion resistance in addition of light weight; bicycle components, rock climbing equipment, inline skating-frames and hang glider airframes are common applications. At first, Al 7075 alloy was developed secretly in Japan in the year of 1943, by Sumitomo Metal. Mandal et al. [1] used a Taguchi laser beam machining system and an Al 7075 alloy sheet to study the effects of laser micro-machining. To

optimise Kerf Width, HAZ and surface roughness, three laser parameters were used: laser beam power, pulse frequency, and scanning speed. When cutting 1.7 mm thick 22MnB5 ultra high strength steel with a CO2 laser, Tahir et al. [2] used RSM to predict the minimal Kerf Width and HAZ in relation to laser power, cutting speed, and duty cycle. Duty cycle is revealed to be the most important factor. The result was a high Kerf Width and thick HAZ due to an increase in laser power and slower cutting speeds. Ghosal et al. [3] utilized RSM to optimize hole

taper and Material Removal Rate (MRR) in laser machining of Al/Al₂O₃-MMC of 2 mm thickness using Ytterbium laser machine (YLR 1000). MRR increased with a reduction in wait time and an increase in laser power, whereas pulse width increased hole taper. Parthipan et al. [4] synthesized, studied and experimented on Cu-Ni-Ti₂ composite material to optimize its MRR and surface roughness using RSM against laser energy, speed and gas pressure. Noor et al. [5] developed first and second-order models using Box-Behnken Design of RSM to predict the surface roughness in CO₂ laser cutting of acrylic sheet of 3 mm thickness. Both models demonstrated that the most important factors in influencing the surface roughness are the power demand and tip distance. Gautam et al. [6] performed experiments to investigate the effects of erbium-doped laser cutting of a woven roving carbon fibre reinforced plastic (CFRP) using Response Surface Method (RSM). Surface roughness and HAZ were calculated after conducting experiments using Optical microscope (BX51M) and Surface Roughness Tester (SJ210). It was observed that with the increase of laser power, decrease in SOD and scan speed; surface roughness and heat affected zone were increased.

Pramanik et al. [7] investigated the effect of sawing angle in laser machining of Ti6Al4V superalloy by Multi diode fibre laser using RSM. Regression model of kerf deviation using RSM was optimized and compared with experimental results. It revealed that with the increase in sawing angle; Kerf Width was increased which led to greater kerf deviation. Mathew et al. [8] performed

experimental study to analyse effect of laser machining parameters using Nd:YAG laser on drilling ability of CFRP using RSM. It was found that the high beam intensity and better focusing of pulsed Nd:YAG laser gave smaller thermal load during cutting which helped in cutting the composite with minimal defects. When laser cutting 4130 steel using RSM, Rajaram et al. [9] examined the effects of laser power and feed rate on Kerf Width, surface roughness, and HAZ width. Dubey et al. [10] utilized a hybrid experimental design based on Taguchi Methodology (TM) and RSM to perform multi-objective optimization for laser cutting of high silicon-alloy steel thin sheet. To increase MRR and reduce top Kerf Width, assist oxygen pressure, pulse width, pulse frequency, and cutting speed were optimised.

2. EXPERIMENTAL PROCEDURE AND OBJECTIVE

Al 7075 alloy is used as the workpiece in the current research project. Al 7075 alloy consists of zinc as the primary alloying element along with magnesium, copper, chromium, iron and few other elements. Here, Nd:YVO₄ fibre laser is used to perform laser machining of Al 7075 alloy. The process parameters selected for this experiment are Laser Beam Power (LBP), Pulse Frequency (PF) and Scanning Speed (SS) and the responses are Kerf Width (KW) and heat affected zone (HAZ). The Design of Experiment (DoE) is conducted in Minitab 18 software followed by RSM. Experimental process layout of the laser micro-machining performed is shown in Fig. 1.

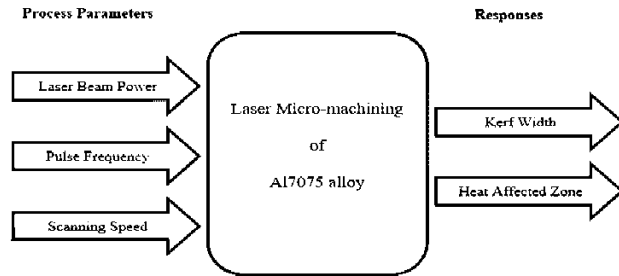


Fig. 1 : Experimental Process Layout

3. RESPONSE SURFACE METHODOLOGY

A collection of statistical and mathematical methods known as Response Surface Methodology (RSM) can be used to create, enhance, and optimise processes. It investigates the connections between several explanatory factors and one or more

response factors. In 1951, George E. P. Box and K. B. Wilson introduced this technique [11]. A Central Composite Design (CCD) model, considering default alpha value, i.e., 1.682, is used which converts a 3-level design into a 5-level design, as shown in Table 1.

4. RESULTS AND DISCUSSION

Using the CCD in DoE section, RSM identified the central and boundary values and created a model consisting of 20 combinations. The 20 points consisted of 6 axial points, 6 central points and 8 corner points of the cube. Experiments are conducted based on CCD following RSM and thereby responses are determined based on respective combinations of process

Table 1: Detail of Process Parameters Using CCD

Parameters	Levels				
	-2	-1	0	+1	+2
Laser Beam Power (LBP)	63.18	70	80	90	96.81
Pulse Frequency (PF)	63.18	70	80	90	96.81
Scanning Speed (SS)	0.81	1.5	2.5	3.5	4.18

Table 2: Detail of Experimental Results

SI. No.	LBP (W)	PF (kHz)	SS (mm/sec)	KW (μm)	HAZ (μm)
1	70	70	1.5	64.44	120.06
2	90	70	1.5	77.22	127.16
3	70	90	1.5	77.28	115.75
4	90	90	1.5	82.97	138.75
5	70	70	3.5	56.36	95.56
6	90	70	3.5	60.37	93.72
7	70	90	3.5	57.78	84.41
8	90	90	3.5	58.69	102.58
9	63.18	80	2.5	56.75	87.89

10	96.81	80	2.5	65.82	107.95
11	80	63.18	2.5	61.41	100.22
12	80	96.81	2.5	67.61	102.99
13	80	80	0.81	83.41	136.77
14	80	80	4.18	55.89	83.66
15	80	80	2.5	63.4	103.64
16	80	80	2.5	61.73	103.39
17	80	80	2.5	61.23	102.45
18	80	80	2.5	63.13	102.91
19	80	80	2.5	63.13	103.06
20	80	80	2.5	62.53	103.24

4. 1. Main Effects Plot

The relationship between each input parameter and each output parameter is depicted by the main effects plot. The plot shows how much the value of a particular output parameter varies with the change in the value of a particular input parameter.

Fig. 2 and Fig. 3 show the main effects plot for Kerf Width and heat affected zone respectively. It has been found that as laser beam power increases, both Kerf Width and HAZ steadily rise. Higher laser beam power causes more heat to be generated, more heat to be dispersed across the machined area, and more metal to be melted and evaporated, increasing the Kerf Width and HAZ.

As Scanning Speed increases, both Kerf Width and HAZ decreases gradually because as the travel of laser beam increases, the amount of heat input and heat spread on the machined region is less, thus reducing the amount of vaporization of metal surface and resulting in a lower Kerf Width and HAZ.

The Kerf Width and HAZ initially fall slightly as

the pulse frequency rises because there is less heat spreading due to the shorter pulse duration. However, as the rise continues, more heat is introduced into the machined area, which causes Kerf Width to increase substantially more than HAZ.

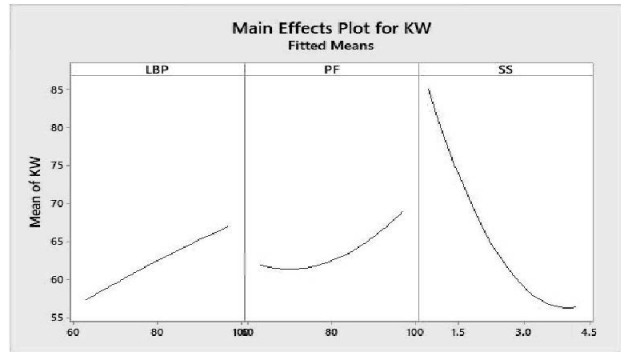


Fig. 2: Main Effects Plot for kerf width

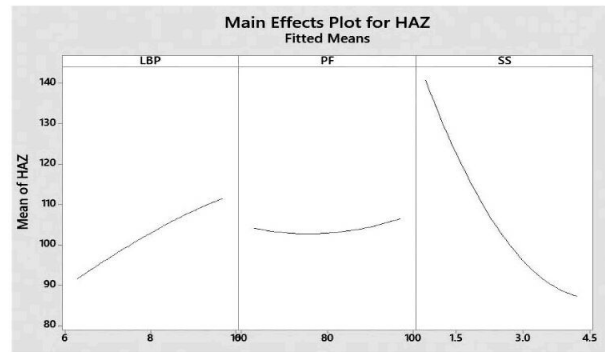


Fig. 3: Main Effects Plot for HAZ

4.2. Response Surface Plot

The combined effect of two process parameters on each individual response parameter, while maintaining the third parameter as constant, is shown in 3D surface plots.

The combined effects of pulse frequency and laser beam power on Kerf Width and HAZ are depicted in Fig. 4 and Fig. 5 respectively, with the scanning speed parameter remained constant at 2.5 mm/sec. It has been discovered that Kerf Width and HAZ increase together with increasing laser beam intensity and pulse frequency. The heat input onto the job surface and heat distribution over the machined region increased significantly as a result of an increase in laser beam power and pulse frequency, which led to more metal evaporation than proper cutting. As a result, as Laser Beam Power and Pulse Frequency increase, so do Kerf Width and HAZ.

The combined impact of scanning speed and laser beam power on Kerf Width and HAZ is depicted in Fig. 6 and Fig. 7 respectively, where the value of Pulse Frequency is held constant at 80 kHz. Kerf Width and HAZ are seen to rise as laser beam power increases, whereas they decrease as scanning speed increases. Metal vaporization occurs as a result of increased heat input onto the metal surface brought on by an increase in laser beam power. But as the laser moves more quickly, less heat is dispersed across the surface as a result of the increased scanning speed. As a result, as scanning speed and laser beam power rise, Kerf Width and HAZ also decrease.

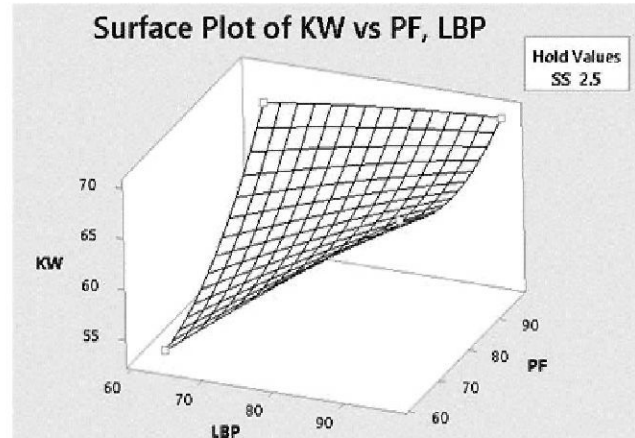


Fig. 4: Surface Plot for kerf width vs PF and LBP

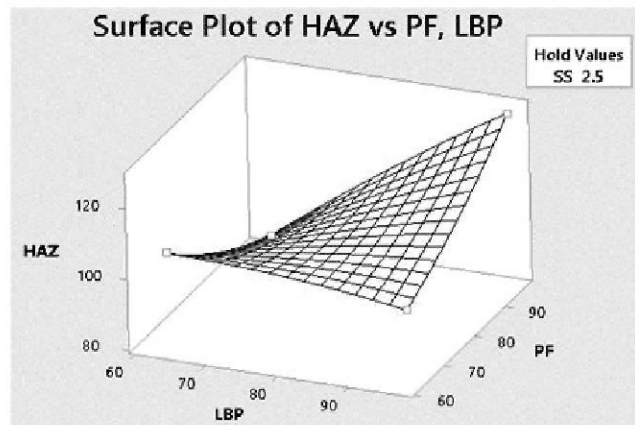


Fig. 5: Surface Plot for HAZ vs PF and LBP

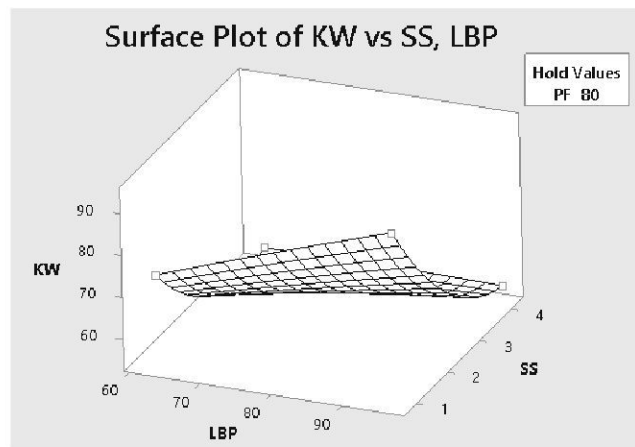


Fig. 6: Surface Plot for kerf width with SS and LBP

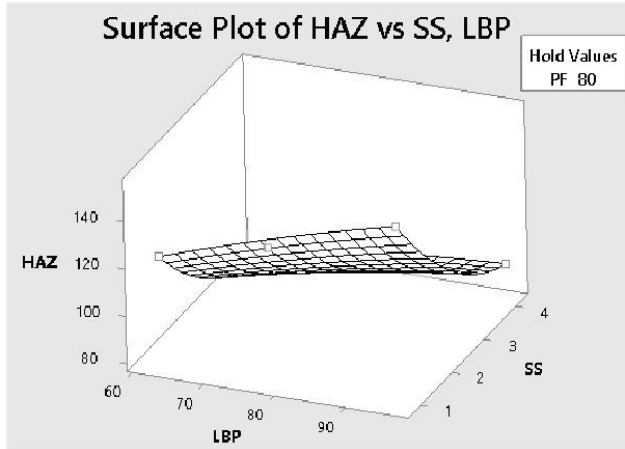


Fig. 7: Surface Plot for HAZ with SS and LBP

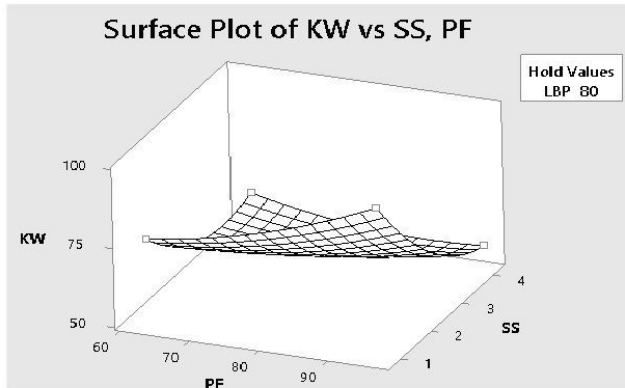


Fig. 8: Surface Plot for kerf width with SS and PF

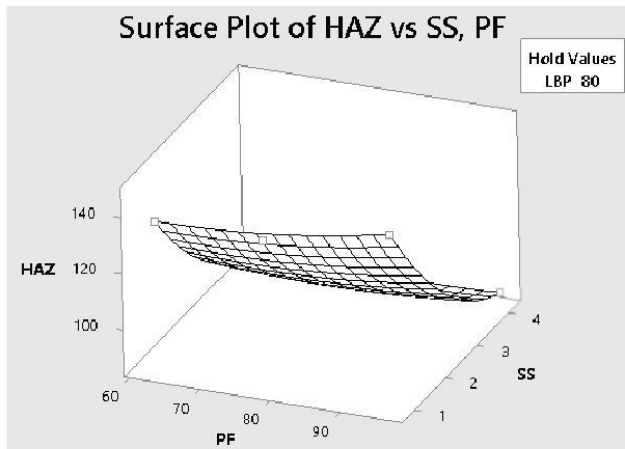


Fig. 9: Surface Plot for HAZ with SS and PF

The combined impact of scanning speed and laser beam power on Kerf Width and HAZ is depicted in Fig. 6 and Fig. 7 respectively, where the value of Laser Beam Power is held constant at 80 W. According to Fig. 8, Kerf Width increases as pulse frequency increases while decreasing as scanning speed increases. The heat input onto the metal surface increased as the pulse frequency rose, causing metal to vaporize. However, as scanning speed increases, less heat is dispersed across the surface. Fig. 9 shows that HAZ falls significantly with an increase in scanning speed but nearly stays constant with an increase in pulse frequency. The quantity of heat dispersed over the surface decreased as scanning speed increased. As a result, as Pulse Frequency and Scanning Speed rise, Kerf Width and HAZ decrease.

4.3. Regression Equations

The second order regression equations of each response are obtained following RSM using Minitab 18 software. The equations obtained are:

$$\text{Kerf Width (KW)} = - 41.1 + 1.893 * \text{LBP} + 0.162 * \text{PF} + 9.72 * \text{SS} - 0.00105 * \text{LBP} * \text{LBP} + 0.01035 * \text{PF} * \text{PF} + 2.853 * \text{SS} * \text{SS} - 0.01274 * \text{LBP} * \text{PF} - 0.1694 * \text{LBP} * \text{SS} - 0.2356 * \text{PF} * \text{SS}.$$

$$\text{Heat Affected Zone (HAZ)} = 366 - 1.83 * \text{LBP} - 4.56 * \text{PF} - 11.8 * \text{SS} - 0.00466 * \text{LBP} * \text{LBP} + 0.00837 * \text{PF} * \text{PF} + 3.881 * \text{SS} * \text{SS} + 0.0449 * \text{LBP} * \text{PF} - 0.172 * \text{LBP} * \text{SS} - 0.120 * \text{PF} * \text{SS}.$$

4.4. Optimization

• Single Objective Optimization

The objective is to minimize Kerf Width and HAZ. Minitab 18 programme is used to carry out the single-objective optimization of Laser Beam Power, Pulse Frequency, and Scanning Speed. The optimum values of process parameters and responses at 100% confidence level, i.e., composite desirability of 1, are shown in Table 3 and Fig. 10 and 11, respectively.

• Multi- Objective Optimization: Using the Minitab 18 programme, the Laser Beam Power, Pulse Frequency, and Scanning Speed single objective optimization is carried out. The optimum values of process parameters and responses at 94% confidence level are shown in Table 4 and Fig. 12.

Table 3: Solution for Single-Objective Optimization of kerf width and HAZ using RSM

LBP	PF	SS	KW Fit	HAZ Fit
96.817	96.817	4.181	52.256	
63.182	96.817	4.181		68.585

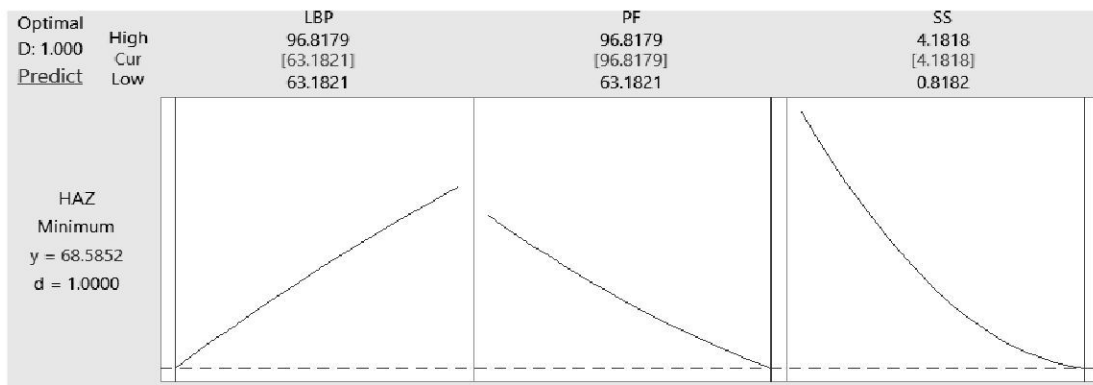


Fig. 10: Optimal parametric combination and response value for kerf width

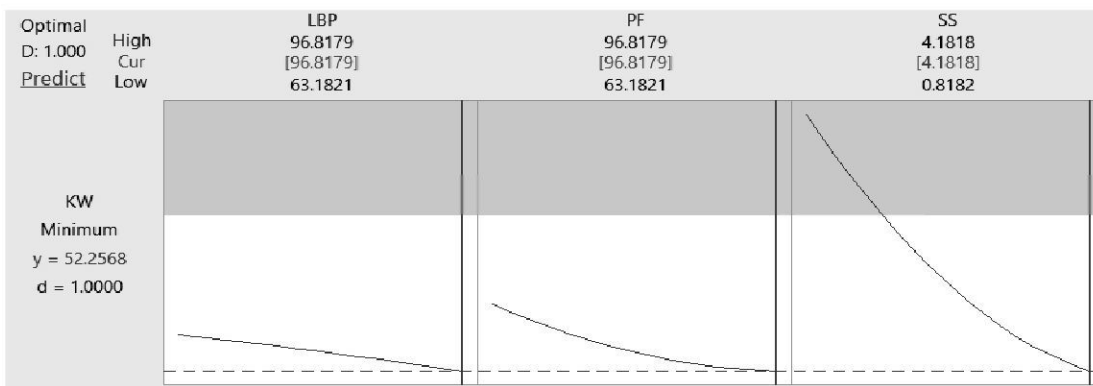


Fig. 11: Optimal parametric combination and response value for HAZ

Table 4: Solution for Single-Objective Optimization of kerf width and HAZ using RSM

LBP	PF	SS	KW Fit	HAZ Fit
63.182	79.181	3.5	54.5678	83.2515

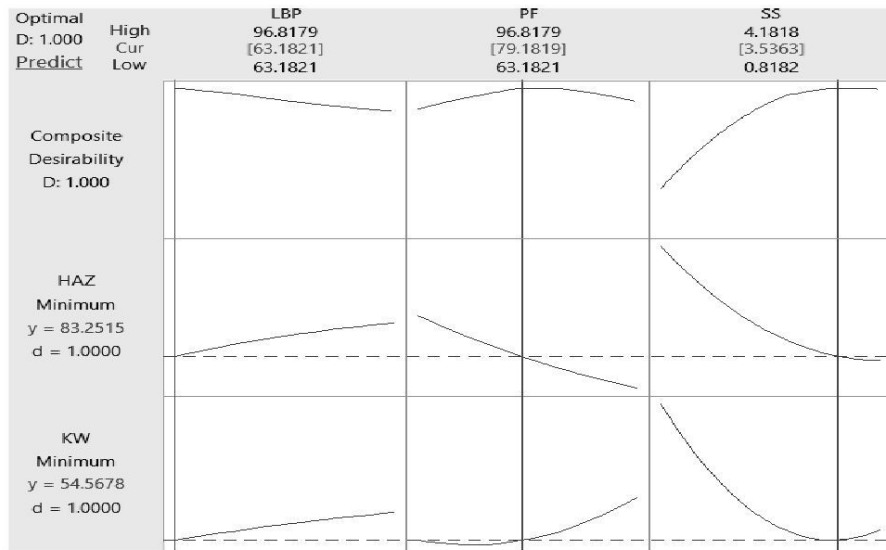


Fig. 12: Optimal parametric combination and response value for kerf width and HAZ

5. CONCLUSIONS

At the end of research work on laser micromachining of Al 7075 alloy, following conclusions can be made:

- Scanning Speed has the most significant effect on both Kerf Width and Heat Affected Zone followed by Laser Beam Power and Pulse Frequency.
- Kerf Width increases with the increase in Laser Beam Power and Pulse Frequency; whereas, it decreases with increase in Scanning Speed.
- Heat Affected Zone increases with the increase in Laser Beam Power and decreases with increase in Scanning Speed.
- Effect of change in Pulse Frequency for both responses is low.

- Combination effect of Laser Beam Power and Pulse Frequency tends to Kerf Width increase, combination effect of Pulse Frequency and Scanning Speed leads to Kerf Width decrease, and combination effect of Laser Beam Power and Scanning Speed tends to Kerf Width decrease.
- Combined effect of Laser Beam Power and Pulse Frequency leads to HAZ increase, combined effect of Pulse Frequency and Scanning Speed decreases HAZ, combined effect of Laser Beam Power and Scanning Speed tends to HAZ decreases.

REFERENCES

[1] Mandal, K. K., Kuar, A.S. and Mitra, S., Experimental investigation on laser

- micromachining of Al 7075 Alloy, *Optics and Laser Technology*, Vol. 107, pp. 260-267, 2018.
- [2] Tahir, A. F. M. and Aqida, S. N., An investigation of laser cutting quality of 22MnB5 ultra high strength steel using response surface methodology, *Optics and Laser Technology*, Vol. 92, pp.142-149, 2017.
- [3] Ghosal, A., Manna, A. and Patil, P., Optimization Process during Laser Machining of 2 mm Thick Al/Al₂O₃ MMC, *Materials Science Forum*, Vol. 900, pp. 121-126, 2017.
- [4] Parthipan, N. and Ilangkumaran, M., Material synthesis, characterization and performance measurement of laser drilling for stir casted Cu-Ni-TiB₂ metal matrix, *Materials Today: Proceedings*, Vol. 6, pp. 1-9, 2019.
- [5] Noor, M.M., Kadirgama, K., Rahman, M.M., Zuki, N.M., Rejab, M.R.M., Muhamad, K.F. and Mohamed, J.J., Prediction Modelling of Surface Roughness for Laser Beam Cutting on Acrylic Sheets, *Advanced Materials Research*, Vols. 83-86, pp 793-800, 2009.
- [6] Gautam, P. and Singh, K. K., Experimental investigation and modelling of heat affected zone and surface roughness in erbium-doped fiber laser cutting of CFRP composite, *Materials Today: Proceedings*, Vol. 5, pp. 24466–24475, 2018.
- [7] Pramanik, D., Goswami, S., Kuar, A. S., Sarkar, S. and Mitra, S., A Parametric Study of Kerf Deviation in Fiber Laser Micro Cutting on Ti6Al4V Superalloy, *Materials Today: Proceedings*, Vol. 18, 3348–3356, 2019.
- [8] Mathew, J., Goswami, G. I., Ramakrishnan, N. and Naik, N. K., Parametric studies on pulsed Nd: YAG laser cutting of carbon fibre reinforced plastic composites, *Journal of Materials processing technology*, Vol. 89, pp. 198-203, 1999.
- [9] Rajaram, N., Sheikh-Ahmad, J. and Cheraghi, S. H., CO₂ laser cut quality of 4130 steel, *International Journal of Machine Tools and Manufacture*, Vol. 43, pp. 351–358, 2003.
- [10] Dubey, A. K., and Yadava, V., Multi-objective optimisation of laser beam cutting process, *Optics and Laser Technology*, Vol. 40, pp. 562-570, 2008.
- [11] Myers, R. H., Montgomery, D. C. And Anderson-Cook, C. M., *Response Surface Methodology. Process and Product Optimization Using Designed Experiments*, John Wiley and Sons, Inc., Third Edition, 2009.